Computer Methods and Programs in Biomedicine 191 (2020) 105382

Contents lists available at ScienceDirect

Computer Methods and Programs in Biomedicine

journal homepage: www.elsevier.com/locate/cmpb

Medical decision making for 5D cardiac model: Template matching technique and simulation of the fifth dimension

Houneida SAKLY[a,*], Mourad SAID[b], Syrine RADHOUANE[c], Moncef TAGINA[a]

[a] COSMOS Laboratory -National Institute of Computer Sciences (ENSI), University of Mannouba, Tunisia
[b] RSNA Member and Chief of the Radiology and Medical Imaging Unit within the International Center Carthage Medical, Tourist Area "JINEN EL OUEST"-5000 Monastir, Tunisia
[c] Private Higher School of Engineering and Technology (Esprit), Technological Pole, Tunisia

ARTICLE INFO

Article history:
Received 29 August 2019
Revised 18 January 2020
Accepted 2 February 2020

Keywords:
5D model
Blood flow, Prognosis
Cardiac pathologies
Valvulopathies

ABSTRACT

The purpose of this paper is to develop a 5D cardiac model which is inspired from the 5D model for the lungs. This model depends on five variables: the anatomical structure of the 3D heart, temporal dimension and the function of blood flow as the fifth dimension. To test this hypothesis, we took the same mathematical modeling as a reference for the fifth dimension of pulmonary flow where $\vec{\mathbf{r}}_{\rho}(\mathbf{t}) = \vec{\mathbf{r}}_{\mathbf{v}}(\mathbf{t}) + \vec{\mathbf{r}}_{\mathbf{f}}(\mathbf{t})$ where $\vec{\mathbf{r}}_{\mathbf{v}}(\mathbf{t})$ is the displacement vectors with approximate magnitudes by linear functions of the tidal volume and $\vec{\mathbf{r}}_{\mathbf{f}}(\mathbf{t})$ is the blood flow. The scans were acquired for 10 patients,in the 404 series for a total of 18,483 images studied in three cases: healthy patient, case of heart failure and aortic stenosis. Where $\vec{r}_v$ and $\vec{r}_f$ are the unit vectors along the volume of ejection and the blood flow axes, indicating the direction of motion of the object due to heart volume ejection and blood flow variations, respectively. The quantities of α and β coefficients are determined from real-time patient image data. The alpha and beta coefficients are derived from the following dimension equations[mm / ml] [mm*ms / ml] . Since the cardiac system has two diastolic and systolic phases, we have calculated α_1 and β_1 for telediatolic volume and α_2 and β_2 for telesystolic volume throughout the cardiac cycle as a function of the location of the cuts chosen randomly.

Fifth-dimensional experiments are used to track, simulate the behavior of blood flow to detect preliminary indications for the identification of stenosis or valve leakage. The average discrepancy was tabulated as the global fraction of systolic ejection. The results shown in Fig. 3 detect a correspondence between the hunting chamber cut and the flow sequence through the orifice of aorta for this patient with suspicious of having an aortic stenosis disease and an ejection fraction about 71% with a maximum of velocity (Vmax) detected=250 (cm / ms) = 2.5 (m / 10–3 s). In this case this patient has a minor stenosis in the aorta. It should be referred that the normalization of this measures is classified such as : Minor stenosis: area 1.5 cm2, Vmax <3 m / moderate stenosis: area 1.0 - 1.5 cm2, Vmax 3 - 4 m / severe stenosis: area <1.0 cm2, Vmax> 4 m / s. For a patient who has an aortic stenosis the cloud of the points is accumulated comparing to the origin of the axis while the patient with a symptom of insufficiency the points are widened with a remarkable gap in the trajectory.

To solve the issue of the bad prediction, the inaccuracy of the clouds points of the model 5D, the lack of the exact measurements to estimate the degree of cardiac insufficiency (leakage or stenosis), a solution of 5D imagery was depicted. Our main contribution is to test the validity of the template-matching algorithm and the fifth dimension simulation to provide more clues to detect the aortic stenosis and cardiac insufficiency in the context of medical decision support.

1.Introduction

The first definition of the template matching titled the hit-or-miss transform (HMT) was introduced by Matheron [1] and Serra [2]. This technique has been extended to gray level images, this leads to several definitions that are unified by Naegel et al. [3]. The

* Corresponding author.
E-mail addresses: houneida.sakly@esiee.fr (H. SAKLY), mouradsaid@yahoo.fr (M. SAID), syrine.radhouane@esprit.tn (S. RADHOUANE), moncef.tagina@ensi-uma.tn (M. TAGINA).

https://doi.org/10.1016/j.cmpb.2020.105382
0169-2607/

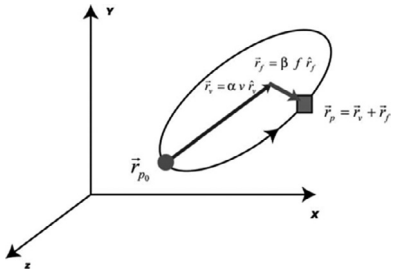

Fig. 1. Mathematical characterization of heart motion (shown as circle in reference breathing phase $\vec{r}_{p0}$ at and square at arbitrary phase at the point$\vec{r}_p$) for cardiac cycle. Tidal volume and blood flow indicated by υ and ŧ, respectively. $\vec{r}_v$ and $\vec{r}_f$ vector is tidal volume and blood flow displacement vector, respectively.

choice will become difficult among the many solutions available[4]. The operator is necessary to make the configuration such as the structuring functions is really useful in practice. Nevertheless, extensions of gray-scale images to multivariate images causes an inherent difficulty in properly configuring the transformation and its parameters which decrease its operational interest in practice. Weber et al. [5]. propose a new, more intuitive operator that allows morphological correspondence of models in multivariate images both spatially and spectrally. This technique is used for flow trajectory tracking. An example presented by Xin et al. [6]. for the detection of velocities and flow trajectories in solid. Wang et al. [7]. use this method for the bubble tracking and bubble rising velocity in wave transformation. In fact, template matching is also a very topical issue in a wide range of medical image applications. To face with the diversity of quantity, quality, size of the images currently produced by the different modalities, several automatic tools are arranged to extract the necessary and useful information to make the medical diagnosis. Among these tools, model matching methods aim to extract relevant information from different images for a specific patient. This technique is used in a framework of proposition of a decision-making approach, Connolly and al [8]. use the template matching method in neurovascular which gathers the activity of the brain and the subsequent change in blood flow to the active region to detect This methodology allows to take some measurements and metrics for the monitoring and the change of burst. The work of Zhang et al. [9]. aims to assist in surgical planning and to provide image guidance in coronary artery treatments from 3D cardiac CT sequences using template matching. Although this technique seeks to identify and group the similarity points between different images for medical diagnosis, this approach is limited in terms of accuracy in locating of these common characteristics for some types of images that are not acquired under the same conditions. The requirement to apply this type of algorithm for images that have at least the same structure and morphology makes this a pointless approach for some cuts in a cardiac examination.

In this context, this paper aims to adopt to test the reliability of the template matching technique in order to quantify the blood flow in valves applied in 4D cardiac sequence with MRI coupled with its study of 2D blood flow. By analogy and following the work proposed by Low et al.[10]., which presents a 5D mathematical model for the monitoring and detection of the lung tumor in lungs and the template matching technique which shows the maximum volume of the lungs. The goal of this work is to test viability of this theory for the identification of cardiopathies and more precisely the heart failure syndromes such as valvulopathies.

This paper is organized as follows: the next section presents the mathematical model for the simulation of the fifth dimension of flow and the materials. Section 3 to list the results obtained with the template matching algorithm and the simulation of the fifth dimension of the blood flow and we finalized by Section 4 for the

Table 1
Realted work for different field of medical imagery.

Proposed by	Cutrale et al. [11]	Huang et al. [12]	Vamvakeros et al. [13]	Heist et al. [4]	Low et al. [10]	Sigfridsson et al. [14]	Feng et al. [15]	Sakly et al. [16]
Field of research	Biomedical imagery	Microscopic imagery	Tomographic diffraction imagery	Hyperspectral imagery	Lung imagery	Cardiac and lung imagery	Cardiac and lung imagery	Cardiac imagery
3D	coordinates (x,y,z)	coordinates (x,y,z)	coordinates (x,y,z)	coordinates (x,y,z)	coordinates (x,y,z)	coordinates (x,y,z)	coordinates (x,y,z)	coordinates (x,y,z)
4D	Time (t)	Time (t)	Diffusion dimension	Time (t)	Time(t)	Respiratory time for the lungs	Time(t)	Time (t)
5D	(λ) wavelength	multi-fluorescence channel	(time / imposed state)	wavelength R (λi))	Air flow (f(t_f)	(Systole and diastole) Time for cardiac cycle	Respiratory dimension	Blood Flow (t_f)

Table 2
Reated work for cardiac imagery.

5D Model	Dimension	Approach	Acquisition condition
Low et al.,2005 [10]	3D lung volume + time + air flow (t)	Template matching	Irregular breathing cycles
Sigfridsson et al., 2007 [14]	3D heart volume + two temporal dimensions, similarly (t heart + *t* lungs)	Reconstruction	Respiratory with arbitrary heart phase
Feng et al.,2017 [15]	Cardiac volume 4d + respiratory dimension	Reconstruction	Respiratory with arbitrary heart phase
Proposed Model, Sakly et al., 2019 [16]	3D cardiac volume + time + blood flow	Reconstruction and rigid registration	Apnea

discussion of this results and their impact on the diagnosis and a perspective for the future work.

2. Methods and materials

2.1. Methods

To test the 5D hypothesis, which has been proposed by [Low et al.] in 2005 for the first time and did not prove effective for detecting abnormalities in the lungs without the intervention of the heart system for cardiac imaging, we take the following mathematical model

$$\vec{r}_{\rho}(t) = \vec{r}_{v}(t) + \overrightarrow{r_f} \quad (1)$$

The displacement vector $\vec{r}_{\rho}(t)$ is the sum of two displacement vectors$\vec{r}_{v}(t)$ and $\overrightarrow{r_f}$. We suppose that these two independent functions are $\overrightarrow{r}_{v}(t)$ (the volume of the heart) and $\overrightarrow{r_f}(t)$ (the blood flow) . The linear model is used to describe $\overrightarrow{r}_{v}(t)$, $\overrightarrow{r_f}(t)$ as follows:

$$\vec{r}_{v} = \alpha \text{ v } \overrightarrow{r_v} \quad (2)$$

$$\vec{r}_{f} = \beta \text{ f } \overrightarrow{r_f} \quad (3)$$

Where $\vec{r}_{v}$ and $\vec{r}_{f}$ are the unit vectors along the volume of ejection and the blood flow axes, indicating the direction of motion of the object due to heart volume ejection and blood flow variations, respectively. The quantities of α and β coefficients are determined from real-time patient image data. The alpha and beta coefficients are derived from the following dimension equations[mm / ml] [mm*ms / ml] . Since the cardiac system has two diastolic and systolic phases, we have calculated α_1 and β_1 for telediatolic volume and α_2 and β_2 for telesystolic volume throughout the cardiac cycle as a function of the location of the cuts chosen randomly.

The 5D model is summarized by five variables was described as following: the coordination of the heart object (anatomical structure), telediastolic and telesystolic volume during a complete cardiac cycle, and the corresponding blood flow ŧ (t) during the cardiac cycle.

The dependence of cardiac movement (diastole and systole) on these five dimensions was insufficient to characterize the whole cycle quantitatively. Linear modeling was also necessary to test our 5D hypothesis, whose movement due to cardiac volume and blood output were separated. The cardiac cycle model is summarized in Fig. 1:

To validate the 5D hypothesis, we must develop a linear model. This simulates the displacement of a 3D object by separating the information on the tidal volume υ (t) and on the blood flow ŧ (t). It defines the position of a point r_{ρ} at the phase ρ following the model in the Eq. (1).

2.1. Materials

This work is based on a database of 10 patients, which contains the following fields: the endocardial and epicardial volume for 20 phases for each patient, the locations are chosen randomly for different cuts during the cardiac examination with a time delay for each phase.

Three cases of patients was performed : the exam of the first patient (healthy) is acquired with 26 series and 1436 images, the second case (syndrome of aortic stenosis) is acquired with 48 series and 1756 images and last case with heart failure syndrome is acquired with 34 series and 1441 images.

The global parameters calculated by the software ReportCard are the fraction of systolic ejection, the flow compensation, cardiac index, of both telesystolic and telediastolic volume and indexed volume, the global ejection volume, cardiac velocity, the maximum velocity rate and the maximum ejection velocity. The parameters calculated in the database are the Alpha and Beta (α,β) parameter for the endocardial and epicardial volume and the module of the displacement vector relative to the ejection volume as well as the vector of displacement relative to the flow $\overrightarrow{r}_{v}$ and $\vec{r}_{f}$.

Data that is extracted directly from the tags of image wich are useful for this study (Field of View “FOV”, “Thickness” Thk, Location “Loc”, Time Repetition”TR”, Time Echo”TE”, Number of Excitation ‘NEX’) needed to describe the 60 and 20 degrees of freedom inherent in the average of 20 locations for each patient.

3. Overview of the methods

An accurate cardiac model is described by acquiring 3D and 4D sections with 2D blood flow sequences under the apnea phase acquired by MRI for the prognosis of cardiac pathologies and valvulopathies. Based on real-time measurements (ejection fraction (%), average displacement / location (mm), endo-cavitary and epicardial heart volume (ml), flow compensation (bmp), telediastolic and telesystolic heart volume, ejection speed and filling of blood flow…) which are acquired during the cardiac examination and from the physiological function of the heart.

The 5D model for the lungs introduced by [Low et al., 2005] inspired a 5D cardiac concept. The diversification of the 5D concept depends on the area of research and the impact of adding a fifth dimension for each approach as shown in Table 1.

By focusing on the field of cardiac imaging, the definition of the fifth dimension remains ambiguous as well as the modeling differs by comparing the approach acquired and the acquisition conditions mentioned in Table 2.

Our contribution focuses on our published research in to describe the 5D concept, which consist to define: the anatomical structure of 3D heart, the time dimension is an implicit variable in this model and the function of the fifth dimension blood stream.

The main objective is to perform the reliability of the 5D heart system (3D heart volume + *t* + blood flow) independently of the respiratory system with the Template Matching technique and analyze their impact on medical diagnosis. In the second linker, it is to cite the limits of this approach and to enhance our solution model compared to the work that has been developed in Table 2.

Table 3
Steps of template matching algorithm.

Template matching algorithm: inputs (hunting chamber, sequence of study of blood flow), outputs (detect the common features in both of images)
1-Read Template image (hunting chamber) and target image (blood flow sequence)
2-Apply template matching using power of the image
•Check which one is target and which one is template using their size
•find both images sizes
•correlate both images sizes and calculate the mean of image part under mask
3-Apply template matching using DC components of the image (the average of all the samples in the window)
•Check which one is target and which one is template
•Read both images sizes
•Calculate the mean of the template
•Corrolate both images
•Extract the mean of image part under mask

4. Results

4.1. Template matching

The algorithm shown in Table 3 has been implemented with MATLAB to detect the similarity point between the hunting chamber section and its flux study. The flow sequences make it possible to code the phase of the signal in proportion to the speed of flow of the blood flow. That is to say that on the reconstructed phase image, the tone in the image will be dark when the flow flows in one direction and in clear when the flow is done in the opposite direction. This principle being applied to a cine sequence, the image series thus makes it possible to visually assess the topographic distribution and the kinetics of the flow. Speed encoding can be done perpendicular to the plane of the hunting chamber [17].

This approach consists in defining the image template and the target image by comparing their dimension first, calculate the average of the pixels of the template, generate a mask for this template and extract the correlation matrix for the two images. To implement template matching two functions are used, as a result, the program can find the template image inside the target image using correlation.

After the application of the template-matching algorithm for 4D cardiac sequences shown in Fig. 2 and their flow study shown in Fig. 3 for a patient suspicious of having a moderate stenosis in the aorta.We obtained the following results in Fig. 4:

The results shown in Fig. 3 detect a correspondence between the hunting chamber cut and the flow sequence through the orifice of aorta for this patient with suspicious of having an aortic stenosis disease and an ejection fraction about 71% with a maximum of velocity (Vmax) detected=250 (cm / ms) = 2.5 (m / 10–3 s). In this case this patient has a minor stenosis in the aorta. It should be referred that the normalization of this measures is classified such as [17]: Minor stenosis: area 1.5 cm2, Vmax ⟨3 m / moderate stenosis: area 1.0 - 1.5 cm2, Vmax 3 - 4 m / severe stenosis: area <1.0 cm2, Vmax⟩ 4 m / s.

By tracking and repeating the template-matching algorithm, we could detect an index for the maximum velocity of flow found in the flush chamber cut as shown in Fig. 5.

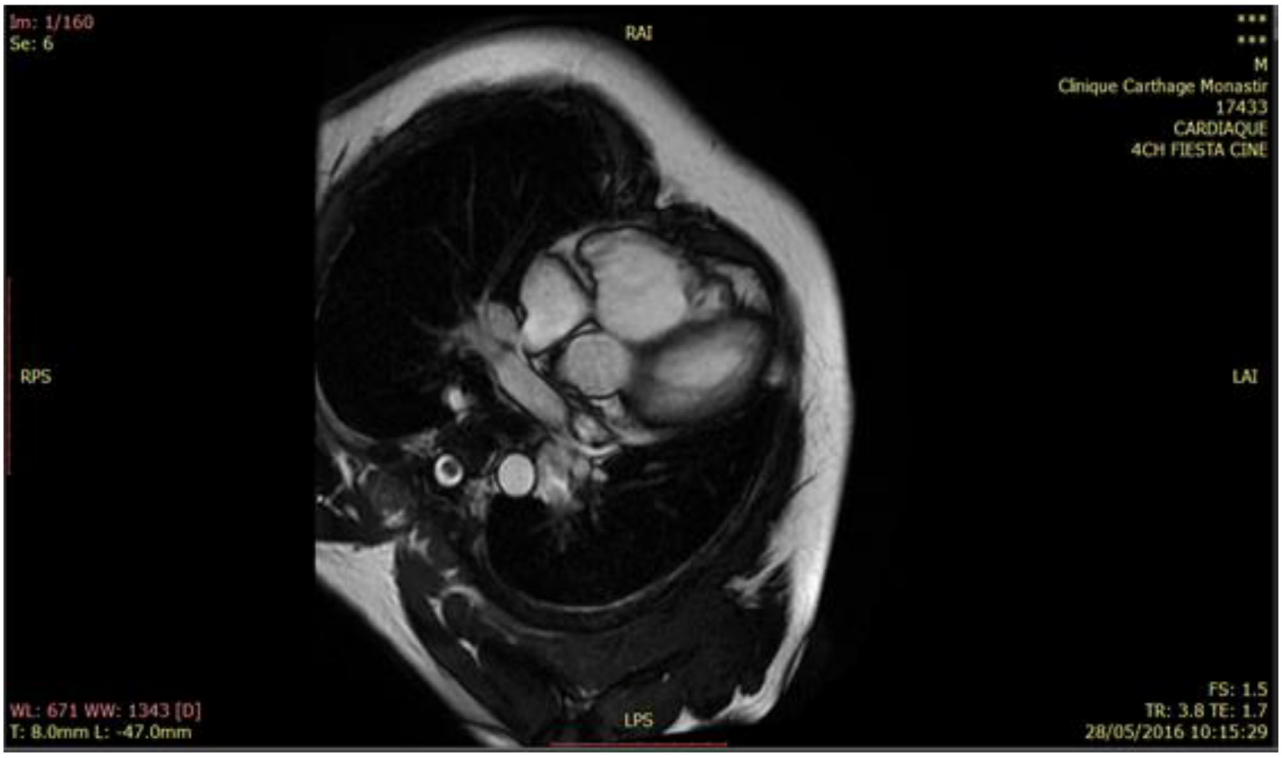

Fig. 2. Cardiac sequences 4D (1/60);FOV=380 mm,Thk=8 mm,Loc=−47 mm,TR=3.8 ms,TE=1.7 ms,NEX=1presented in 60 degrees of freedom.

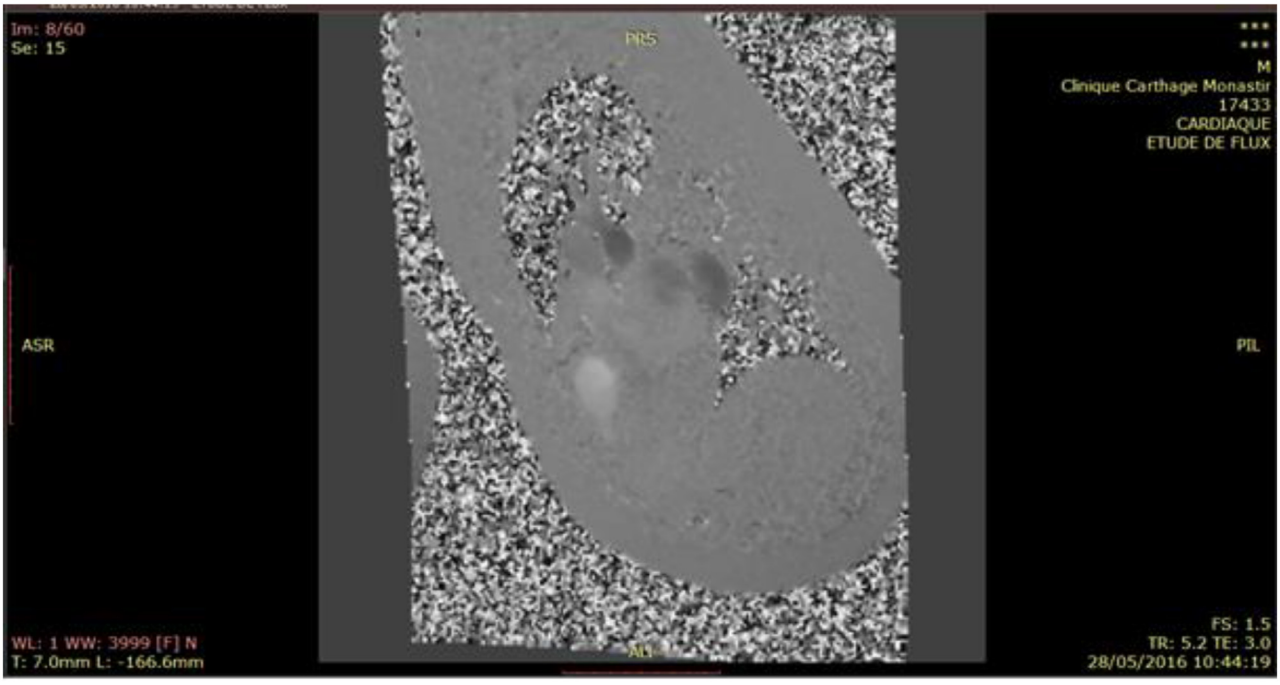

Fig. 3. Sequence (8/60) of the blood flow; FOV=420 mm, Thk=7 mm, Loc=−166.6 mm, TR=5.2 ms, TE=3 ms, NEX=1presented in 20 degrees of freedom.

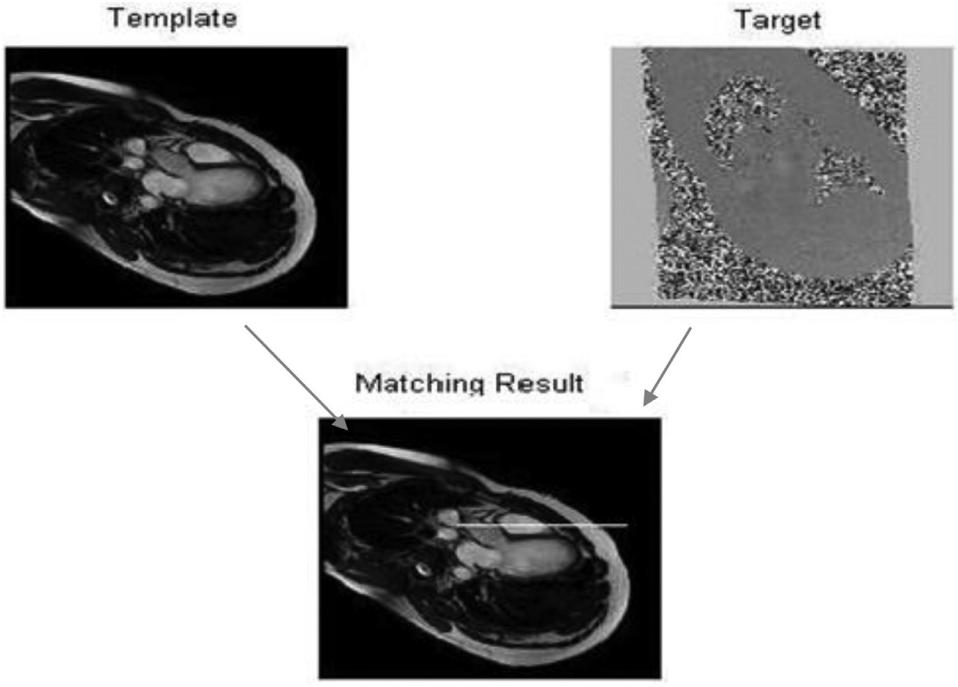

Fig. 4. Result of Template Matching Algorithm.

4.1.1. Model limitation

In fact, we limited this approach of template matching in these two cuts, as we cannot get the flow sequences through the hunting chamber. This strategy can give us some clues about the volume of the flow that is in the hunting chamber section and subsequently an assessment of the diameter of the aortic valve orifice that can induce to an estimation of the degree of stenosis.

The inconvenient of this solution is that it is hard to quantify the flow in the aortic or mitral valve in the left ventricle and that it is not possible to visualize the direction of incoming and outgoing blood flow. The lack of parameters following this algorithm makes the step of prognostic very delicate.

Otherwise, this solution suffers from another weakness: it is the difficulty of estimating the fraction of regurgitation, that is to say the ratio: (retrograde flow / anterograde flow $\times$ 100%) for the patients, which have cardiac insufficiency, and subsequently the extraction of measures for pathology, will be very limited.

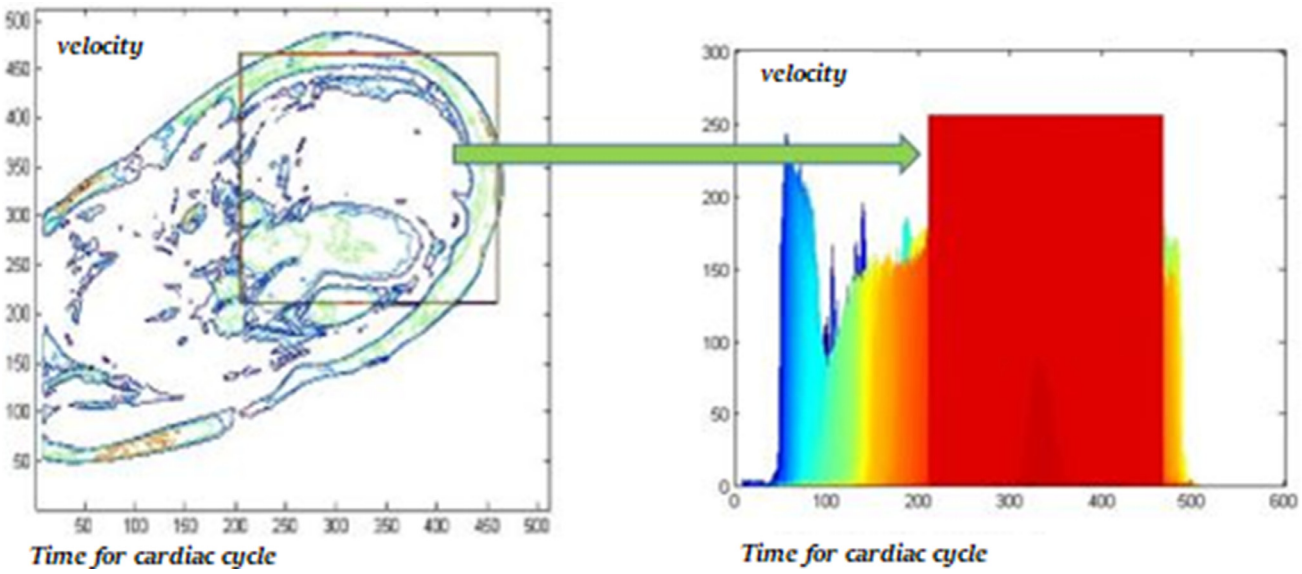

Fig. 5. Maximum velocity detected in the hunting chamber .

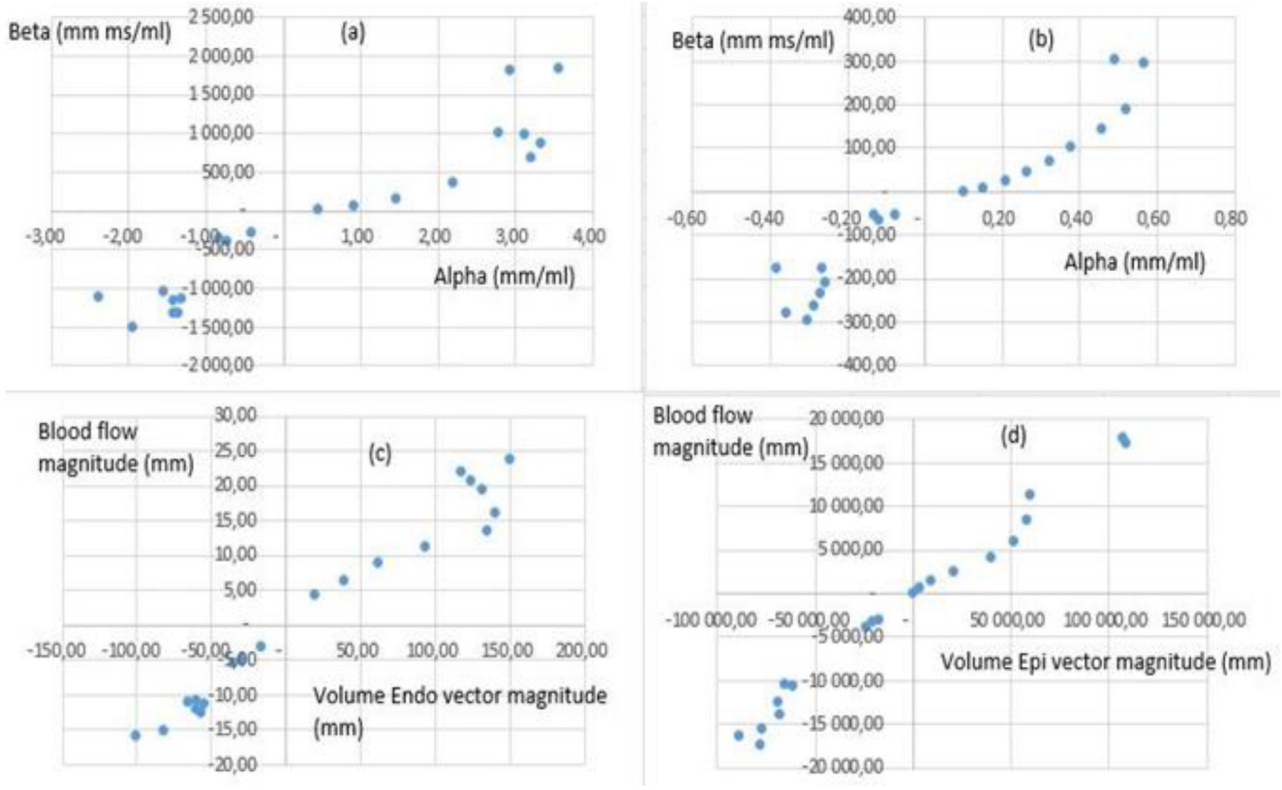

Fig. 6. case study for a healthy patient with systolic ejection fraction rate 64.3%: (a): Tidal endocardial volume versus flow coefficients;(b) Tidal epicedial volume versus flow coefficients,(c) Flow displacement vs endocardial volume displacement,(d) Flow displacement vs pericardial volume displacement.

4.2. Simulation of the fifth dimension

The motion of blood flow in the heart during apnea has been demonstrated as a function of five degrees of freedom, location of cuts for a phase for endocardial and epicardial volume and blood flow. The positions have been parametrized by two vectors, the current global ejection volume and the blood flow. Displacement along these vectors was proportional to tidal volume and blood flow. This model was applied to areas in the heart of three patients: a healthy patient and a case of aortic stenosis and cardiac insufficiency symptoms with MRI. We calculated the Alpha and Beta parameters according to the following equation [mm / ml], [mm*ms / ml], respectively. The estimation of these coefficients for the endocardial and epicardial volume is shown in Fig. 6, Fig. 7 and Fig. 8 for the three cases with systolic ejection fraction rate 64.3%, 71%, 53.7% respectively. These results were not satisfied to the experts as seen the hard task of prediction of the rate of leakage or stenosis rate. This model can give signs or symptoms of aortic stenosis or heart failure via the distribution of clouds points from the origin. The weak points of this model is reflected through the

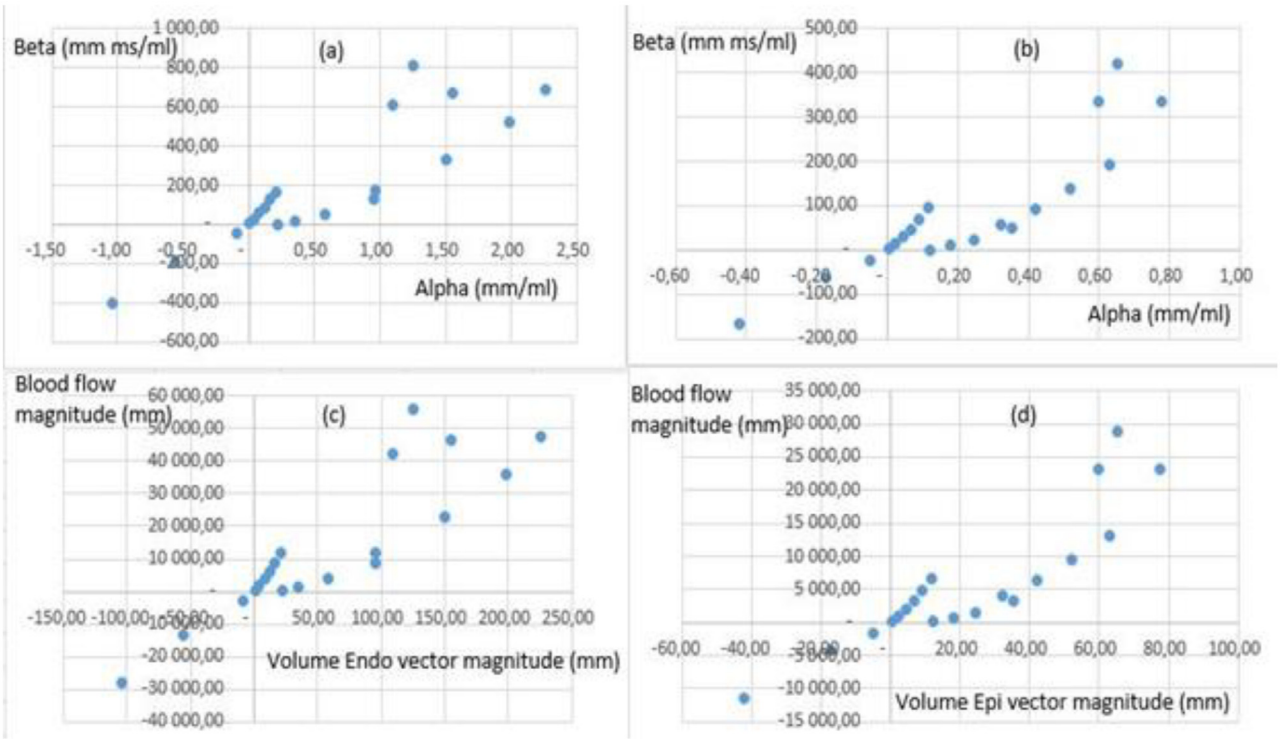

Fig. 7. case study of aortic stenosis symptoms patient with systolic ejection fraction rate 71% (a): Tidal endocardial volume versus flow coefficients;(b) Tidal epicedial volume versus flow coefficients,(c) Flow displacement vs endocardial volume displacement,(d) Flow displacement vs pericardial volume displacement.

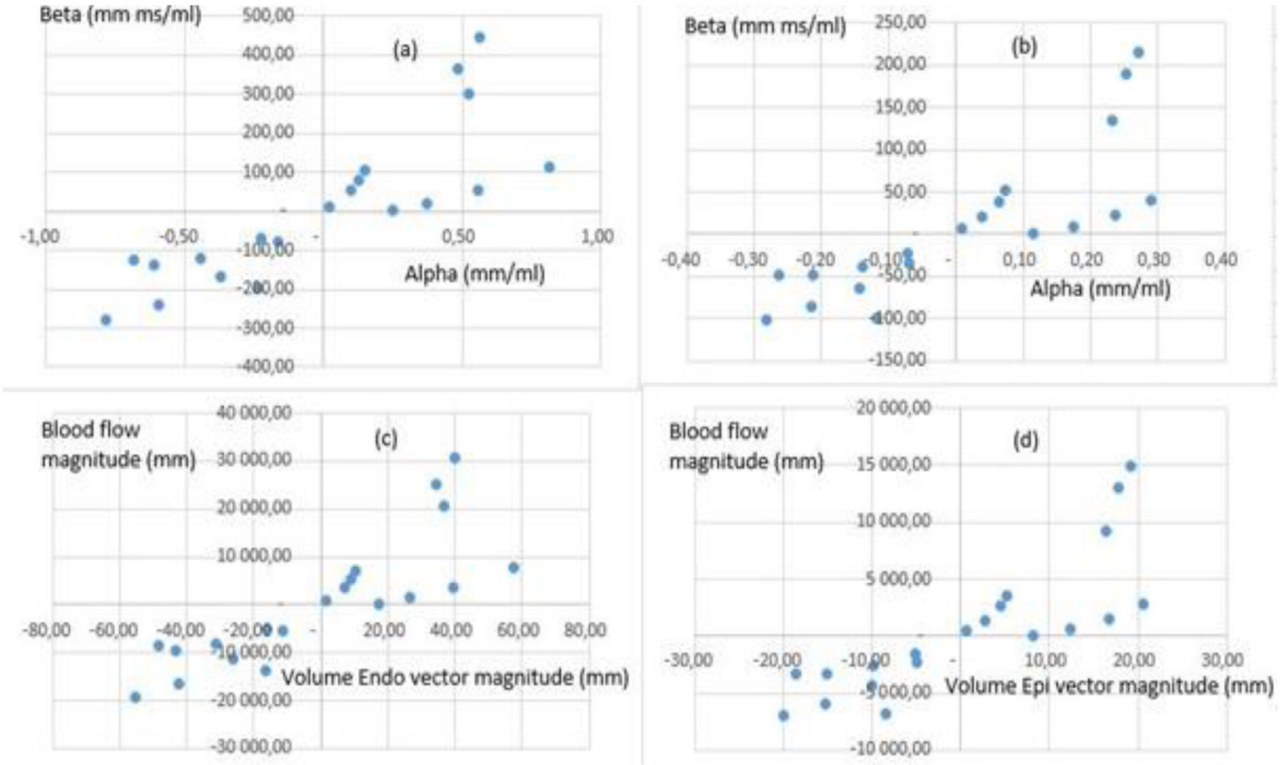

Fig. 8. case study of cardiac insufficiency a patient with systolic ejection fraction rate 53.7% (a): Tidal endocardial volume versus flow coefficients;(b) Tidal epicedial volume versus flow coefficients,(c) Flow displacement vs endocardial volume displacement,(d) Flow displacement vs pericardial volume displacement.

location of the cuts that depends on the quality of acquisition, the position it takes the patient during the exam. This parameter has been chosen randomly in different sequences without respecting the order of acquisition as seen in Table 4. Therefore, if we repeat the same simulation, we cannot guarantee to have the same results given the choice of localization.

This approach is mainly to guide the experts for the non-critical cases who have cardiac anomaly syndrome: aortic stenosis and cardiac failure. The results of the proposed 5D model simulation were not accurate to take the right medical inference. These results show the interest for the fifth dimension to identify heart insufficiency or aortic stenosis .We note that the cloud of points of the coefficients Alpha and Beta for a healthy patient are located on trajectory in a balanced way. This can give an idea of the localization of the flow based on the distribution of cloud point comparing to the endocardial and epicardial volume during a cardiac cycle that has been processed during 20 phases. We cannot conclude a definitive medical inference in the case of patients who have systolic ejection fraction between [50% −75%] versus the simulations of the patient who has a syndrome of aortic stenosis or heart failure. For a patient who has an aortic stenosis the cloud of the points is accumulated comparing to the origin of the axis while the patient with a symptom of insufficiency the points are widened with a remarkable gap in the trajectory. In conclusion, this concept shows the benefits of integrating the blood flow dimension into the medical decision-making stage, but this method remains not accurate to crucial evaluation based on the ejection fraction for the detection of genital diseases if it exceeds to 70% and for cardiac insufficiency, especially for the case of valvulopathies if it is less than 50% [18].

5. Discussion

The technique of template matching proposed by the [Low] model is an unsatisfactory technique for the therapeutic needs to identify the valvular pathology and to detect and follow the trajectory and the direction of the fluid in the cut of the flush chamber according to the results mentioned above. Useful for the assessment of medical diagnosis and quantification of the outflow and the inflow and subsequently extracting measures to classify the severity of valvular pathology. Among the techniques used to provide information on the trajectory and flow direction is Biomarkers [19] and fluorescence imaging [20]. The choice of the appropriate method to satisfy this condition depends on the medical context.

The 5D model was able to predict the type of valvular pathology desired across linear trajectories. Non-linear motion behavior arises from the nonlinear temporal dependence of the overall ejection volume. If the model is stable over time, it proves to be an exciting breakthrough in characterizing the blood flow movement. Modeling the fifth dimension as a function of the phase space of the tidal volume rather than time coupled with real-time measurements of the heart volume could provide the clinician with an accurate determination of the real-time flow movement in a volume Cardiac 4D.

The proposal for such a fifth-dimensional modeling for an internal cardiac system remains limited in relation to the works [15] [14], that proposed integrating a respiratory dimension for 4D cardiac images. If the model is fundamentally correct in its physical properties, the coefficients and the blood flow and the volume vectors of the model must be varied according to the location of the cardiac sequences taking account the consideration of (axial cut, long axis, 4 cavities, short -axis …) . Therefore, interpolation of the model parameters will be possible and the behavior of the model as a function of position could be used to determine the endocardial and epicardial volume by examining the divergence of blood flow movement in a cardiac contour.

Table 4
Example of calculated measurement applied in 5D modeling for the first case study (patient with aortic stenosis syndrome).

PATIENT N°	PHASE (n)	AVERAGE DEPLACEMENT (mm)/localisation	TDEL ms	VOLUME ENDO LV (ml)	VOLUME EPI LV(ml)	Flow C (bmp)	Velocity (ml)	beta1	alpha1	beta2	alpha2	rv1	rv2	rf1	rf2
1	1	28,6	10	130,3	237,3	69	99,9	2,19	0,22	1,21	0,12	21,93	12,04	151,45	83,16
	2	41,6	52	117,3	230,9			18,44	0,35	9,37	0,18	35,43	18,00	1 272,47	646,43
	3	54,6	94	93,8	222,2			54,72	0,58	23,10	0,25	58,15	24,55	3 775,43	1 593,77
	4	67,6	136	70,9	190,5			129,67	0,95	48,26	0,35	95,25	35,45	8 947,23	3 329,97
	5	55,6	179	57,9	173,1			171,89	0,96	57,50	0,32	95,93	32,09	11 860,37	3 967,16
	6	68,6	221	45,7	162,7			331,74	1,50	93,18	0,42	149,96	42,12	22 890,18	6 429,51
	7	81,6	263	41	156,8			523,43	1,99	136,87	0,52	198,83	51,99	36 116,96	9 443,85
	8	94,6	305	41,9	150,6			688,62	2,26	191,59	0,63	225,55	62,75	47 514,49	13 219,50
	9	−27,6	348	49,8	159,4			−192,87	−0,55	−60,26	−0,17	−55,37	−17,30	- 13 307,86	- 4 157,66
	10	−70,92	390	68,4	168,2			−404,37	−1,04	−164,44	−0,42	−103,58	−42,12	- 27 901,42	- 11 346,36
	11	139,46	432	90	179,5			669,41	1,55	335,64	0,78	154,80	77,62	46 189,15	23 158,91
	12	1,06	474	106,8	193,1			4,70	0,01	2,60	0,01	0,99	0,55	324,61	179,54
	13	−10,1	517	117,3	206,4			−44,52	−0,09	−25,30	−0,05	−8,60	−4,89	- 3 071,59	- 1 745,63
	14	140,39	559	127,9	234,7			613,59	1,10	334,38	0,60	109,66	59,76	42 337,63	23 071,93
	15	5,38	601	130,9	236,3			24,70	,04	13,68	0,02	4,11	2,27	1 704,38	944,15
	16	161,1	643	128,3	247,4			807,38	1,26	418,70	0,65	125,44	65,05	55 709,46	28 890,56
	17	10,94	686	133	253			56,43	0,08	29,66	0,04	8,22	4,32	3 893,49	2 046,77
	18	16,93	728	140,7	258,5			87,60	0,12	47,68	0,07	12,02	6,54	6 044,26	3 289,86
	19	22,91	770	139,1	252,9			126,82	0,16	69,75	0,09	16,45	9,05	8 750,60	4 813,00
	20	28,9	812	139,4	246,9			168,34	0,21	95,05	0,12	20,71	11,69	11 615,56	6 558,16

The proposed model could also be predictive. The data examined showed that the model was precise for the proceed treated cases during which the data were acquired from the images. The accuracy of this day model depends on the location of the patient. 5D modeling as a function of the 3D tidal heart volume coupled with the real time dimension as well as heart volume measurements, which could provide the clinician with an accurate determination of movement in real time.

At this stage, we will move towards improving the proposed equation with the addition of specific terms to describe the tracking of blood flow via the use of diffusion kurtosis imaging (DKI) and diffusion tensor imaging (DTI) [25] [26].

6. Conclusion

In this paper, we depict a strategy for medical decision diagnosis in cardiac imaging with MRI. This approach stipulates to conceive a 5D model, which depends on five dimension: anatomical structure of the heart in 3D, temporal dimensions as well as a functional dimension of blood flow for the detection of stenosis and valvular regurgitation. To solve the issue of the bad prediction, the inaccuracy of the clouds points of the model 5D, the lack of the exact measurements to estimate the degree of cardiac insufficiency (leakage or stenosis), a solution of 5D imagery was depicted.

Our main contribution is to test the validity of the template-matching algorithm and the fifth dimension simulation to provide more clues to detect the aortic stenosis and cardiac insufficiency in the context of medical decision support

Our future work will be based on the proposal of a registration technique for the detection of fluid in a cardiac volume while respecting the elasticity characteristics of the fluid [21] [22], [23], [24],. For the visualization of the flow direction and to quantify the retrograde and anterograde flow we propose to exploit the DTI [25]and DKI [26] scattering tensors and to study their impact on the mediated diagnosis for valvulopathies. Long-term goals is to solve the equation of Naviers-stokes for a laminar and viscous blood fluid to have the final model 5D (3D+time+flow). The extraction of measurements (field of the vortex, masses of flow, static pressure, Reynolds number) based on the fifth dimension is used to identify the area and the degree of stenosis. With the increasing demand for high-resolution simulations, it has become important to study the cost and response time of digital solvers that can take advantage of recent architectures including multi-core processors. In future work, we propose to simulate an efficient solver for the resolution on heterogeneous CPU / GPU architectures of Navier-Stokes (NS) equations relating to flows of incompressible fluids

Declarations

All authors took the authorization for the use of the database for the submission of the paper «5D cardiac model: template matching technique and simulation of the fifth dimension" and the IRB / ethics approval was not required for this study.

Availability of data and material

The datasets generated and/or analysed during the current study are not publicly available due [Private accesses of the Radiology and Medical Imaging Unit within the International Center Carthage Medical] but are available from the correspond ing author on reasonable request

Declaration of Competing Interest

The authors declare that they have no competing interests.

Acknowledgments

We would like to acknowledge the Carthage International Medical Center that supported this work and to the medical staff for providing the blind data used in this study.

Funding

No finding received for this research work.

Supplementary materials

Supplementary material associated with this article can be found, in the online version, at doi:10.1016/j.cmpb.2020.105382.

References

[1] J.F.C. Kingman, Review: G. Matheron, random sets and integral geometry, Bull. Amer. Math. Soc. 81 (1975) 844–847.
[2] J. Serra, Image analysis and mathematical morphology, Academic Press, Inc., Orlando, FL, USA, 1983.
[3] B. Naegel, N. Passat, C. Ronse, Grey-level hit-or-miss transforms-Part I: unified theory, Pattern Recogn. 40 (2007) 635–647, doi:10.1016/j.patcog.2006.06.004.
[4] E. Aptoula, S. Lefèvre, A comparative study on multivariate mathematical morphology, Pattern Recognit. 40 (2007) 2914–2929, doi:10.1016/j.patcog.2007.02.004.
[5] J. Weber, S. Lefèvre, Spatial and spectral morphological template matching, Image Vis. Comput. 30 (2012) 934–945, doi:10.1016/j.imavis.2012.07.002.
[6] L. Xin, L. Lizheng, Solid-fluid velocity detection algorithm based on template matching, in:, in: 27th Chinese Control Conference, 2008, pp. 192–195, doi:10.1109/CHICC.2008.4605017. 2008.
[7] H. Wang, F. Dong, A effective image matching method for bubbly flow based on wavelet transform, in:, in: 2nd International Congress on Image and Signal Processing, 2009, pp. 1–5, doi:10.1109/CISP.2009.5303643. 2009.
[8] M. Connolly, P. Vespa, X. Hu, Characterization of cerebral vascular response to EEG bursts using ICP pulse waveform template matching, Acta Neurochir. Suppl. 122 (2016) 291–294, doi:10.1007/978-3-319-22533-3_58.
[9] D.P. Zhang, L. Risser, C. Metz, L. Neefjes, N. Mollet, W. Niessen, D. Rueckert, Coronary artery motion modeling from 3D cardiac CT sequences using template matching and graph search, in:, in: IEEE International Symposium on Biomedical Imaging: From Nano to Macro, 2010, pp. 1053–1056, doi:10.1109/ISBI.2010.5490171. 2010.
[10] D.A. Low, P.J. Parikh, W. Lu, J.F. Dempsey, S.H. Wahab, J.P. Hubenschmidt, M.M. Nystrom, M. Handoko, J.D. Bradley, Novel breathing motion model for radiotherapy, Int. J. Radiat. Oncol. Biol. Phys. 63 (2005) 921–929, doi:10.1016/j.ijrobp.2005.03.070.
[11] F. Cutrale, V. Trivedi, L.A. Trinh, C.-.L. Chiu, J.M. Choi, M.S. Artiga, S.E. Fraser, Hyperspectral phasor analysis enables multiplexed 5D in vivo imaging, Nat. Methods 14 (2017) 149–152, doi:10.1038/nmeth.4134.
[12] Y.S. Huang, H.Y. Ku, Y.C. Tsai, C.H. Chang, S.H. Pao, Y.H. Sun, A. Chiou, 5D imaging via light sheet microscopy reveals cell dynamics during the eye-antenna disc primordium formation in Drosophila, Sci. Rep. 7 (2017) 44945, doi:10.1038/srep44945.
[13] A. Vamvakeros, S.D.M. Jacques, M. Di Michiel, D. Matras, V. Middelkoop, I.Z. Ismagilov, E.V. Matus, V.V. Kuznetsov, J. Drnec, P. Senecal, A.M. Beale, 5D operando tomographic diffraction imaging of a catalyst bed, Nat. Commun. 9 (2018) 4751, doi:10.1038/s41467-018-07046-8.
[14] A. Sigfridsson, J.-P.E. Kvitting, H. Knutsson, L. Wigström, Five-dimensional MRI incorporating simultaneous resolution of cardiac and respiratory phases for volumetric imaging, J. Magn. Reson. Imaging 25 (2007) 113–121, doi:10.1002/jmri.20820.
[15] L. Feng, S. Coppo, D. Piccini, J. Yerly, R.P. Lim, P.G. Masci, M. Stuber, D.K. Sodickson, R. Otazo, 5D Whole-Heart Sparse MRI, Magn Reson Med, 2017, doi:10.1002/mrm.26745.
[16] H. Sakly, R. Mahmoudi, M. Akil, M. Said, M. Tagina, MOVING towards a 5D Cardiac Model, JFV 26 (2019), doi:10.1615/JFlowVisImageProc.2018027194.
[17] O. Vignaux, Imagerie cardiaque : Scanner Et IRM, Second Edition, ELSEVIER MASSON, 2011 https://www.elsevier-masson.fr/imagerie-cardiaque-scanner-et-irm-9782294712258.html accessed April 11, 2017.
[18] J. Bogaert, S. Dymarkowski, A.M. Taylor, V. Muthurangu, Clinical Cardiac MRI, Second Edition, Springer, 2012 http://www.springer.com/cn/book/9783642230349 accessed April 12, 2017.
[19] C.L. Sutphen, A.M. Fagan, D.M. Holtzman, Progress Update, Fluid and imaging biomarkers in Alzheimer's disease, Biol. Psychiatry 75 (2014) 520–526, doi:10.1016/j.biopsych.2013.07.031.
[20] S. Kwon, C.F. Janssen, F.C. Velasquez, E.M. Sevick-Muraca, Fluorescence imaging of lymphatic outflow of cerebrospinal fluid in mice, J. Immunol. Methods 449 (2017) 37–43, doi:10.1016/j.jim.2017.06.010.
[21] H.-.H. Chang, C.-.Y. Tsai, Adaptive registration of magnetic resonance images based on a viscous fluid model, Comput. Methods Programs Biomed. 117 (2014) 80–91, doi:10.1016/j.cmpb.2014.08.004.

[22] E. D'Agostino, F. Maes, D. Vandermeulen, P. Suetens, A viscous fluid model for multimodal non-rigid image registration using mutual information, Med. Image Anal. 7 (2003) 565–575, doi:10.1016/S1361-8415(03)00039-2.
[23] S. Klein, M. Staring, K. Murphy, M.A. Viergever, J.P.W. Pluim, elastix: a toolbox for intensity-based medical image registration, IEEE Trans. Med. Imaging 29 (2010) 196–205, doi:10.1109/TMI.2009.2035616.
[24] S. Ahmad, M.F. Khan, Dynamic elasticity model for inter-subject non-rigid registration of 3D MRI brain scans, Biomed. Signal Process Control 33 (2017) 346–357, doi:10.1016/j.bspc.2016.12.016.
[25] H. Zhu, M. Styner, N. Tang, Z. Liu, W. Lin, J.H. Gilmore, FRATS: functional regression analysis of DTI tract statistics, IEEE Trans. Med. Imaging 29 (2010) 1039–1049, doi:10.1109/TMI.2010.2040625.
[26] R. Loução, R.G. Nunes, R. Neto-Henriques, M. Correia, H. Ferreira, Human brain tractography: a DTI vs DKI comparison analysis, IEEE 4th Portuguese Meeting Bioeng. (ENBENG) (2015) 1–2 2015, doi:10.1109/ENBENG.2015.7088820.